THE ASTROPHYSICAL JOURNAL, 416:62–73, 1993 October 10

PLANETARY NEBULAE AS STANDARD CANDLES. IX. THE DISTANCE TO THE FORNAX CLUSTER

RUSSET MCMILLAN AND ROBIN CIARDULLO[1,2]
Department of Astronomy and Astrophysics, Penn State University, 525 Davey Laboratory, University Park, PA 16802
AND
GEORGE H. JACOBY[1]
Kitt Peak National Observatory, National Optical Astronomy Observatories, P.O. Box 26732, Tucson, AZ 85726
Received 1993 March 8; accepted 1993 April 19

ABSTRACT

We present the results of a planetary nebula (PN) survey of three galaxies in the Fornax Cluster performed with the Cerro Tololo 4 m telescope and on-band off-band [O III] λ5007 interference filters. In all, we detected 224 PN candidates: 105 in the peculiar S0/Sa galaxy NGC 1316 (Fornax A), 47 in the E2 galaxy NGC 1404, and 72 in the central cD of the cluster NGC 1399. Using statistically complete samples of planetaries and the procedures described in previous papers in the series, we derive distances to these galaxies from the planetary nebula luminosity function (PNLF). Our distance moduli of 31.13, 31.17,and 31.15 to NGC 1316, 1399, and 1404 show that the cluster is tightly clumped, as suggested by Tonry (1991). By summing the observed PNLFs of the three galaxies, we calculate a mean cluster distance modulus of 31.14 ± 0.14 (16.9 ± 1.1 Mpc) and estimate a Hubble constant of 75 ± 8 km s^{-1} Mpc^{-1}, in excellent agreement with that determined from PN observations in Virgo. We also compare our PNLF distances to those determined from the D_n-σ method and show that the internal uncertainties estimated by both groups are essentially correct.

Subject headings: distance scale — galaxies: clusters: individual: Fornax — ISM: individual (NGC 1316, 1399, 1404) — planetary nebulae: general

1. INTRODUCTION

The Fornax Cluster of galaxies is a large, well-mixed cluster in the southern hemisphere that is similar to the Virgo Cluster in many respects. Although Fornax is only one-seventh as large as Virgo, both clusters have a sizable population of both spiral and elliptical galaxies and are dominated at their cores by an X-ray bright elliptical galaxy rich in globular clusters. Also like Virgo, Fornax lies beyond the reach of such traditional extragalactic distance indicators as Cepheid and RR Lyrae variables, but within the range of a variety of other techniques, and has been the host of some well-observed Type Ia supernovae. Both clusters are distant enough to show significant velocity due to their Hubble flow, and thus are important landmarks for measuring the Hubble constant. Moreover, since Fornax is 132° from Virgo on the sky, accurate velocity-independent distance measurements to both clusters can reveal much about matter streaming and infall for a large area around the Local Group.

Various investigators have attempted to find the distance to Fornax through different methods. Most find it to be at a distance similar to that of Virgo, but only a few techniques are capable of determining an independent distance to the cluster. Of those, the two most reliable methods, the infrared Tully-Fisher relation (Aaronson et al. 1989) and the surface brightness fluctuation method (Tonry 1991), disagree on the Fornax/Virgo distance ratio by 0.33 ± 0.25 mag. Thus, an improved distance to the cluster is needed for a better understanding of the structure of our local region of space.

The planetary nebula luminosity function (PNLF) is an ideal tool for investigating this discrepancy. Planetary nebulae (PNe) can most easily be identified in the early-type galaxies which define the Fornax Cluster's core, and, since PNe need only be observed at one epoch, it is relatively easy to measure the distances to several galaxies of the cluster. More importantly, previous tests of the method have shown that the PNLF is insensitive to a galaxy's Hubble type and color (Jacoby, Ciardullo, & Ford 1990 [Paper V]; Ciardullo, Jacoby, & Harris 1990 [Paper VII]) and only slightly affected by differences in metallicity (Ciardullo & Jacoby 1992 [Paper VIII]).

In Paper V we used the PNLF to measure a distance of 14.7 ± 1.0 Mpc to six galaxies in the Virgo Cluster core. In this paper, we use the same method to find the distance to three galaxies in Fornax: NGC 1316 (radio source Fornax A), NGC 1399, and NGC 1404. In § 2, we describe our observations and reductions and tabulate the astrometric coordinates and [O III] λ5007 magnitudes of the PNe discovered in our surveys. In § 3, we present the raw PNLFs and review our procedures for defining statistically complete samples of objects. Our most likely distances and bolometric-luminosity specific PN densities are given in § 4. In § 5, we derive the distance ratio between Fornax and Virgo for different samples of galaxies and show that the measured radio depends on the individual objects observed. We then estimate the accuracy of the PNLF and the D_n-σ relation and discuss the implications of our distance to NGC 1316 for the calibration of Type Ia supernovae. We conclude by using our measurement of the distance to Fornax to estimate the value of the Hubble constant.

2. OBSERVATIONS AND REDUCTIONS

The PNLF distance method is most easily applied in early-type galaxies, where variable dust extinction is negligible and the identification of PN candidates through λ5007 emission is

[1] Visiting Astronomer, Cerro Tololo Inter-American Observatory, National Optical Astronomical Observatories, operated by the Association of Universities for Research in Astronomy, Inc., under contract with the National Science Foundation.
[2] NSF Young Investigator.

less likely to be contaminated by high-excitation H II regions. For this reason, two of the three Fornax member galaxies we selected for observation are ellipticals: NGC 1399, the central cD of the cluster, and NGC 1404, its nearby companion. The third galaxy, NGC 1316, is classified as Sap by Sandage & Tammann (1981) based on its dust lanes, as a cD galaxy by Schweizer (1980) based on its total luminosity and surface brightness profile, and as a PLXSOP (a peculiar, semibarred, intermediate lenticular with an S-shape and a pseudo–outer ring) by de Vaucouleurs et al. (1991). The distance to this galaxy is of special interest since it has hosted two well-observed Type Ia supernovae (1980N and 1981D) and is an active galaxy; an independent distance estimate can therefore help calibrate the Type Ia supernova (SN Ia) luminosities and provide information on the energetics of an active galactic nucleus (AGN).

Our survey technique was as described in previous papers. Each galaxy was observed in both a narrow-band filter transmitting ~ 30 Å around the [O III] $\lambda 5007$ emission line (shifted to match the redshift of the galaxy) and a wider off-band filter covering ~ 300 Å in the same spectral region. Typical on-band exposures consisted of three hour-long integrations, while the off-band exposures were generally one-seventh as long.

Observations of the three target galaxies were performed with the prime focus imager of the Cerro Tololo Inter-American Observatory (CTIO) 4 m telescope during runs in 1989 November, 1990 December, and 1991 December. In 1989, observations of NGC 1404 and NGC 1399 were obtained with two different TI CCDs (one failed during the run), both of which afforded a field of view of 4′ and a scale of 0.″3 per pixel. The following year, we attempted to supplement these observations by observing NGC 1316 with a Tektronix 512 CCD, which had a slightly larger field of view (4.′6) and larger pixels (0.″54). Unfortunately, during this run, the seeing was never better than 1.″6; thus, although PNe were detected, the data did not allow us to measure a reliable distance. Therefore, in 1991, we reimaged NGC 1316 and NGC 1399 under better seeing conditions with a Tektronix 1024 CCD, which had an 8′ field of view and 0.″47 per pixel. A log of these observations appears in Table 1. The survey fields are outlined in Figure 1.

Because NGC 1316 is known to have dust lanes and star-forming regions, our 1990 observations of this galaxy also included images through a 75 Å full width at half-maximum (FWHM) Hα filter. Since H II regions generally have Hα/[O III] ratios greater than one, while [O III] bright PNe all have Hα/[O III] < 1, any object visible on both the [O III] narrow-band frame and the Hα frame could be identified as a H II region and excluded from the PNLF. In fact, since we concentrated on identifying PNe in the halo of the galaxy, it was not necessary to discard any of the PN candidates because of Hα emission. For the same reason, we believe that our PN measurements are not affected by variable internal extinction from the galaxy's dust lanes.

The initial identification of PN candidates was performed by blinking sums of several on-band images against the corresponding off-band images. "Difference" images, consisting of summed on-band frames minus their corresponding scaled off-band frames, were also useful in identifying and cross-checking potential candidates. The PN candidates appeared as point sources on the on-band frames, but were completely absent on the off-band frames, and therefore produced a positive point on the otherwise flat difference image.

After first identifying the PN candidates on the summed images, we checked individual on-band frames to ensure that no cosmic rays were included among the candidates. Objects that appeared bright on a single frame but were invisible on the rest of the exposures were discarded from the analysis. For PNe in NGC 1316 and NGC 1399, data from other years provided additional confirmation for the candidates. For both these galaxies, the 1991 frames were the primary source of photometry, since these images had the highest signal-to-noise ratio and field coverage. However, many of the PNe identified on these frames were also visible on images from previous years—the exceptions being objects that fell outside the survey fields of the smaller CCD chips and the faintest PNe, which were near or beyond the completeness limit of the best frames. Thus, objects that appeared quite bright on our deeper 1991 data but were invisible in the frames of earlier years were also deleted from our candidate list. After the spurious images were removed, 105 PN candidates remained in NGC 1316, 72 remained in NGC 1399, and 47 remained in NGC 1404.

In order to calculate the equatorial coordinates of the PN candidates, we imaged each galaxy through a B and V filter with a Thompson 1024 CCD on the CTIO 0.6 m Schmidt telescope. This detector/telescope combination produced frames with a field of view of 31′ and a scale of 1.″8 per pixel. By co-adding a series of five ~ 150 s exposures for each galaxy, we produced images that were both large enough to include 10 or more stars from the *Hubble Space Telescope* (*HST*) Guide Star Catalog and deep enough to show the fainter stars which appeared in the smaller-format 4 m frames. We then measured the equatorial coordinates of these faint field stars by comparing their Schmidt frame positions to those of the *HST* Guide Stars. The PNe coordinates were then calculated in a similar fashion, by comparing their coordinates on the 4 m frames to those of the faint field stars. Based on the rms residuals of our

TABLE 1

SUMMARY OF OBSERVATIONS

Field	Date	Detector	Filter	Exposure (hr)	Temperature	Seeing
NGC 1399 east	1989 Nov 28	TI 1	5027/30	3	16.5	1.″2
NGC 1399 west	1989 Nov 30	TI 2	5027/30	3	16.0	1.3
NGC 1399 center	1990 Dec 19	Tek 512	5027/30	1	17.0	1.4
NGC 1399 center	1991 Dec 6	Tek 1024	5027/30	3	16.5	1.3
NGC 1404	1989 Nov 29	TI 1	5038/30	3	15.5	1.2
NGC 1404	1990 Dec 19	Tek 512	5038/30	1	17.0	1.4
NGC 1316 northeast	1990 Dec 17	Tek 512	5038/30	5	14.5	1.7
NGC 1316 southwest	1990 Dec 18	Tek 512	5038/30	4	17.0	1.7
NGC 1316 center	1990 Dec 19	Tek 512	5038/30	1	17.0	1.4
NGC 1316 center	1991 Dec 5	Tek 1024	5038/30	3	16.0	1.3

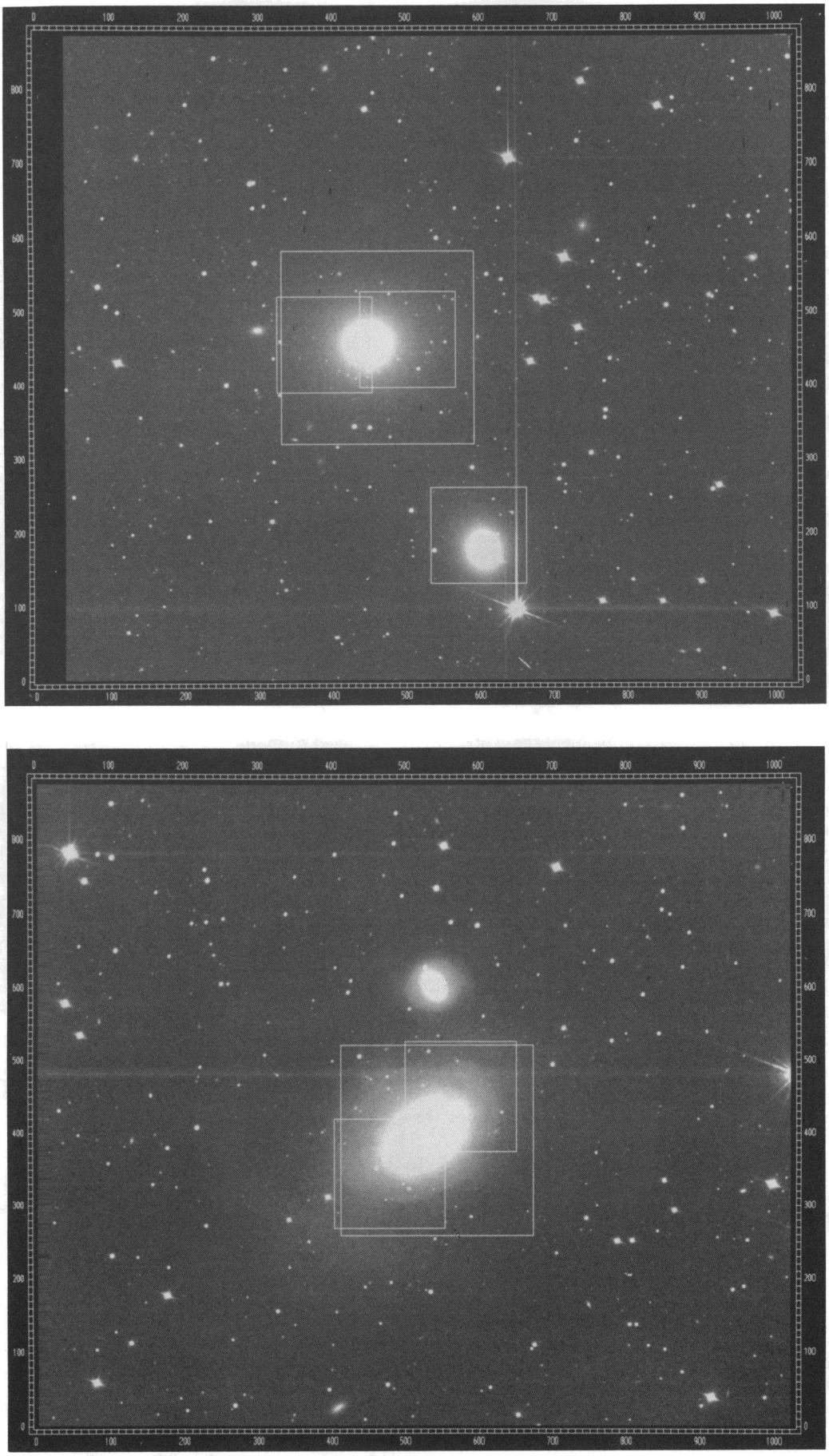

FIG. 1b

FIG. 1.—The survey fields for NGC 1399, 1404, and 1316 are shown overlaid on sections of our Thompson 1024 CCD images taken with the CTIO 0.6 m Schmidt telescope. North is at the top, and east is to the left.

fits to the *HST* Guide Stars, we estimate the errors in our Schmidt frame astrometry to be ~0".4. The relative error between our field star positions and the PNe, as determined from the 4 m frames, is somewhat better than this: ~0".2.

Photometry of the PN candidates was performed as in previous papers. We first used the DAOPHOT photometry package (Stetson 1987) to determine the point spread function (PSF) for each field by measuring several isolated stars on the on-band sum frames. We then used these PSFs to determine the instrumental λ5007 magnitudes of field stars on the on-band frames and PNe on the difference frames. For both NGC 1316 and NGC 1399, field star photometry was done in multiple years, but, because of the poor seeing in 1990, PN photometry in NGC 1316 could only be performed on the 1991 data. For NGC 1399, magnitude measurements from 1989 and 1991 were combined using the SUPERPHOT analysis package (Ciardullo et al. 1987), which tied the CCD fields onto a common photometric system by solving the least-squares condition required to match the magnitudes of field stars in the regions of field overlap. All the stellar and PN magnitudes were then placed on an absolute system by comparing 5" aperture measurements of the field stars with similar measurements made of several Stone (1977), Oke (1974), and Stone & Baldwin (1983) spectrophotometric standards. A comparison of our large-aperture measurements made in 1989, 1990, and 1991 indicates that the error in our photometric zero point is less than 0.03 mag.

For the final step in our reductions, we computed the standard magnitudes for the PNe by modeling the filter transmission curves (Jacoby et al. 1989, Paper III) and using the photometric procedures for emission-line objects described by Jacoby, Quigley, & Africano (1987). The assumed galactic systemic velocities were taken from the Revised Shapley Ames Catalog (Sandage & Tammann 1981), and the envelope stellar velocity dispersions were taken from Franx, Illingworth, & Heckman (1989a) and Jenkins & Scheuer (1980). The filter transmission curves, currected for the f/2.7 beam of the telescope and the temperature of the filter at the telescope, appear in Figure 2. A listing of the properties of our program galaxies is given in Table 2. Because our filters are well matched to the systemic velocities of the galaxies, small errors in the transmission curve or the assumed PN velocity dispersion make very little difference to computed [O III] λ5007 fluxes. We estimate the error introduced by the uncertainty in the filter calibration to be ~0.04 mag.

The equatorial positions, computed [O III] λ5007 magnitudes, and number of observations for the planetaries in NGC 1316, 1399, and 1404 are given in Tables 3, 4, and 5. PNe which are included in our statistical sample, as defined below, are identified with an "S." Following Paper II,

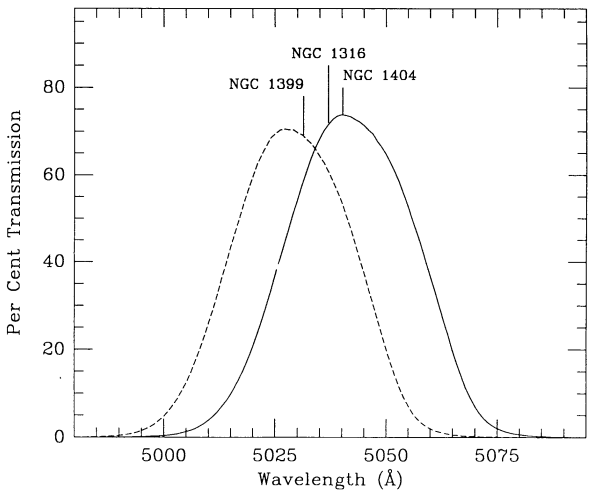

FIG. 2.—The transmission curves for the [O III] λ5007 filters used in this survey, corrected for the f/2.7 beam of the telescope and the temperature of the outside air. The dashed line shows the filter used to observe NGC 1399; the solid curve represents the filter used for NGC 1316 and NGC 1404. The systemic velocities of the three galaxies are marked.

$$m_{5007} = -2.5 \log F_{5007} - 13.74 . \quad (1)$$

The mean internal photometric error of these measurements, as determined by DAOPHOT, is given as a function of magnitude in Table 6. (Since the photometric errors for all three galaxies are similar, they have been combined in the table.) Table 7 gives the coordinates of the brightest astrometric standard stars in our fields.

3. DEFINING THE STATISTICAL SAMPLE

Figure 3 shows histograms for the raw planetary nebula luminosity functions observed for NGC 1316, 1399, and 1404. It is immediately apparent that the three galaxies are at roughly the same distance. All three luminosity functions begin at $m_{5007} \sim 26.6$, turn over due to incompleteness at $m_{5007} \sim 27.3$, and have no obvious overluminous objects requiring a modification of the empirical PNLF. The samples, however, are not statistically complete and cannot be analyzed quantitatively. Because the detectability of faint PNe changes with the background surface brightness, the data are somewhat biased by the inclusion of bright objects from the inner galactic regions, where faint PNe are impossible to identify.

In order to select a statistically complete sample of PNe, we began by including only those objects superposed on regions

TABLE 2

PROPERTIES OF PROGRAM GALAXIES

Galaxy	Hubble Type	Velocity (km s^{-1})	B_T^{0a}	$(U-V)_T^{0a}$	Mg_2	$(m_{1550}-V)^b$
NGC 1316.....	Sap	1793	9.31	1.25	0.298[c]	...
NGC 1399.....	E1	1447	10.22	1.46	0.334[d]	2.05
NGC 1404.....	E2	1929	10.88	1.52	0.317[d]	3.30

[a] From the RC3 catalog (de Vaucouleurs et al. 1991).
[b] From Burstein et al. 1988.
[c] From Gorgas, Efstathiou, & Salamanca 1990.
[d] From Davies et al. 1987.

TABLE 3

NGC 1316 PLANETARY NEBULAE

ID	α(2000)	δ(2000)	Number	m_{5007}	Sample	ID	α(2000)	δ(2000)	Number	m_{5007}	Sample
1.....	3h22m45s.43	−37°10′26″.3	2	26.50	S	54.....	3h22m25s.52	−37°09′40″.8	1	27.15	S
2.....	3 22 49.99	−37 10 11.3	2	26.58	S	55.....	3 22 55.81	−37 09 23.4	2	27.16	S
3.....	3 22 49.53	−37 11 22.7	2	26.60	S	56.....	3 22 55.74	−37 12 51.3	2	27.16	S
4.....	3 22 43.42	−37 15 14.3	2	26.76	S	57.....	3 22 45.71	−37 14 14.8	1	27.17	S
5.....	3 22 56.94	−37 15 28.2	1	26.78	S	58.....	3 22 40.19	−37 09 58.0	1	27.17	S
6.....	3 22 31.85	−37 10 17.8	1	26.82	S	59.....	3 22 58.56	−37 14 56.5	1	27.18	S
7.....	3 22 54.08	−37 09 38.5	2	26.83	S	60.....	3 22 27.46	−37 10 47.1	1	27.19	S
8.....	3 22 35.68	−37 12 36.2	2	26.84		61.....	3 22 42.86	−37 10 40.6	1	27.19	S
9.....	3 22 28.50	−37 15 14.9	2	26.85	S	62.....	3 22 32.18	−37 15 39.5	2	27.19	S
10.....	3 22 32.85	−37 15 18.9	2	26.85	S	63.....	3 22 30.92	−37 14 35.2	2	27.20	S
11.....	3 22 50.73	−37 09 51.9	1	26.85	S	64.....	3 22 49.39	−37 09 29.3	1	27.21	
12.....	3 22 34.62	−37 13 09.6	2	26.86		65.....	3 22 24.50	−37 09 50.4	1	27.21	
13.....	3 22 46.49	−37 10 09.3	2	26.87	S	66.....	3 22 55.59	−37 09 18.8	2	27.22	
14.....	3 22 34.04	−37 16 01.0	2	26.88	S	67.....	3 22 48.01	−37 15 29.0	1	27.23	
15.....	3 22 26.64	−37 11 59.5	2	26.92	S	68.....	3 22 26.37	−37 09 46.6	1	27.23	
16.....	3 22 39.26	−37 14 40.9	2	26.93	S	69.....	3 22 58.01	−37 13 15.0	1	27.24	
17.....	3 22 52.52	−37 08 46.8	2	26.93	S	70.....	3 22 35.37	−37 09 38.3	1	27.24	
18.....	3 22 30.47	−37 14 34.0	2	26.94	S	71.....	3 22 33.62	−37 11 47.0	1	27.24	
19.....	3 22 55.55	−37 14 32.5	1	26.96	S	72.....	3 22 30.53	−37 15 06.7	1	27.25	
20.....	3 22 58.80	−37 12 14.0	2	26.97	S	73.....	3 22 46.08	−37 08 53.5	2	27.25	
21.....	3 22 28.00	−37 15 34.1	2	26.97	S	74.....	3 22 30.36	−37 12 49.9	2	27.26	
22.....	3 22 53.54	−37 11 15.8	1	26.98	S	75.....	3 22 43.74	−37 14 26.1	2	27.26	
23.....	3 22 54.14	−37 08 59.7	1	26.98	S	76.....	3 22 53.95	−37 14 21.7	1	27.27	
24.....	3 22 48.60	−37 10 43.2	2	26.98	S	77.....	3 22 28.81	−37 14 43.7	2	27.27	
25.....	3 22 30.55	−37 15 24.5	1	26.99	S	78.....	3 22 36.95	−37 14 13.1	1	27.28	
26.....	3 22 29.57	−37 12 24.5	2	26.99	S	79.....	3 22 50.31	−37 08 44.3	2	27.28	
27.....	3 22 58.12	−37 12 31.6	2	26.99	S	80.....	3 22 53.26	−37 12 36.9	2	27.30	
28.....	3 22 45.25	−37 10 39.3	1	27.00	S	81.....	3 22 59.14	−37 15 15.6	1	27.30	
29.....	3 22 47.18	−37 11 25.5	2	27.01		82.....	3 22 41.53	−37 09 37.5	1	27.30	
30.....	3 22 42.51	−37 15 38.5	2	27.01	S	83.....	3 22 53.35	−37 12 10.5	2	27.31	
31.....	3 22 46.34	−37 09 17.7	2	27.02	S	84.....	3 22 56.53	−37 13 40.1	1	27.32	
32.....	3 22 56.64	−37 11 56.1	1	27.02	S	85.....	3 22 30.18	−37 15 37.1	2	27.33	
33.....	3 22 41.32	−37 10 09.4	2	27.02	S	86.....	3 22 46.23	−37 08 53.5	2	27.34	
34.....	3 22 30.92	−37 11 32.6	1	27.03	S	87.....	3 22 33.04	−37 14 06.2	2	27.35	
35.....	3 22 43.28	−37 10 59.2	2	27.03		88.....	3 22 47.30	−37 15 09.5	1	27.36	
36.....	3 22 49.87	−37 08 53.5	2	27.03	S	89.....	3 22 51.31	−37 08 48.9	2	27.36	
37.....	3 22 43.86	−37 14 36.0	2	27.03	S	90.....	3 22 51.10	−37 14 36.7	1	27.39	
38.....	3 22 54.14	−37 08 50.4	2	27.04	S	91.....	3 22 33.29	−37 11 44.1	2	27.39	
39.....	3 22 32.86	−37 11 25.0	1	27.04	S	92.....	3 22 31.34	−37 09 46.9	1	27.39	
40.....	3 22 28.90	−37 13 55.5	2	27.05	S	93.....	3 22 39.21	−37 15 55.9	1	27.40	
41.....	3 22 40.60	−37 10 10.2	1	27.05	S	94.....	3 22 30.63	−37 11 39.6	1	27.40	
42.....	3 22 44.42	−37 10 20.2	1	27.06	S	95.....	3 22 30.48	−37 12 59.2	1	27.41	
43.....	3 22 40.58	−37 16 03.1	2	27.07	S	96.....	3 22 28.76	−37 13 55.9	2	27.45	
44.....	3 22 30.22	−37 12 33.1	2	27.07	S	97.....	3 22 52.92	−37 12 35.9	1	27.45	
45.....	3 22 32.58	−37 09 31.8	1	27.08	S	98.....	3 22 41.09	−37 09 52.0	1	27.45	
46.....	3 22 33.59	−37 13 42.9	2	27.09	S	99.....	3 22 40.18	−37 08 55.5	1	27.46	
47.....	3 22 52.19	−37 11 29.0	2	27.09	S	100.....	3 22 48.67	−37 09 39.9	2	27.46	
48.....	3 22 51.56	−37 13 46.5	1	27.10	S	101.....	3 22 33.45	−37 13 47.0	2	27.53	
49.....	3 22 32.98	−37 11 37.0	1	27.11	S	102.....	3 22 58.20	−37 09 47.3	2	27.55	
50.....	3 22 42.45	−37 16 26.3	1	27.13	S	103.....	3 22 25.68	−37 15 13.9	2	27.56	
51.....	3 22 40.08	−37 14 25.7	1	27.14	S	104.....	3 22 55.50	−37 10 34.1	2	27.57	
52.....	3 22 44.82	−37 14 19.9	2	27.15	S	105.....	3 22 51.67	−37 10 14.9	2	27.63	
53.....	3 22 58.70	−37 10 10.4	1	27.15	S						

where the galaxy background is unimportant relative to the brightness of the night sky. Because all our runs were on or near New Moon, the sky brightness during our observations was $m_V \sim 21.6$ mag arcsec^{-2} (Allen 1976, p. 134). Thus, by using the surface photometry of Franx, Illingworth, & Heckman (1989b) and Sparks et al. (1991) to select only those PNe located where the galactic surface brightness $\Sigma_V > 22$ mag arcsec^{-2}, we eliminated the principle source of distortion in the PNLF. In NGC 1316, this criterion excluded five PNe with an isophotal radius $r_{iso} < 110''$; in NGC 1399, 10 objects with $r_{iso} < 60''$ were excluded; and in NGC 1404, seven objects with $r_{iso} < 45''$ were eliminated from the analysis.

We next estimated the magnitude limit of our complete sample by combining theoretical estimates of the system throughput and image quality with the expected signal-to-noise ratio of a PN detection. By adding artificial stars to a CCD image of the bulge of M31, Ciardullo et al. (1987) found that incompleteness was only important when the calculated signal-to-noise ratio of the detections was $\lesssim 9$. This result was confirmed by Hui et al. (1993), who used DAOPHOT error estimates on a sample of halo PNe in NGC 5128 to estimate a signal-to-noise ratio of ~ 10 for objects at the completeness limit. For our Fornax observations, we therefore assumed this limiting signal-to-noise ratio and used our seeing measurements and the CTIO detector efficiencies to estimate our completeness limit in each galaxy. For all three galaxies, this

TABLE 4

NGC 1399 PLANETARY NEBULAE

ID	α(2000)	δ(2000)	Number	m_{5007}	Sample	ID	α(2000)	δ(2000)	Number	m_{5007}	Sample
1.....	3h38m26s.92	−35°26′51″.5	1	26.54		37.....	3h38m20s.02	−35°29′56″.9	1	27.17	S
2.....	3 38 26.57	−35 26 46.7	1	26.54		38.....	3 38 40.92	−35 23 55.1	1	27.17	S
3.....	3 38 30.34	−35 23 29.5	1	26.64	S	39.....	3 38 47.13	−35 28 03.1	2	27.17	S
4.....	3 38 24.68	−35 27 40.5	2	26.70	S	40.....	3 38 34.45	−35 25 50.0	2	27.18	S
5.....	3 38 31.71	−35 27 19.7	2	26.75		41.....	3 38 44.49	−35 27 47.9	2	27.18	S
6.....	3 38 27.76	−35 26 22.4	1	26.76		42.....	3 38 18.87	−35 26 02.3	2	27.18	S
7.....	3 38 40.93	−35 27 54.5	2	26.78	S	43.....	3 38 25.76	−35 23 59.3	1	27.18	S
8.....	3 38 23.06	−35 26 39.2	2	26.78	S	44.....	3 38 13.52	−35 29 52.9	1	27.20	S
9.....	3 38 23.79	−35 29 50.4	1	26.81	S	45.....	3 38 34.70	−35 29 15.9	1	27.21	
10.....	3 38 34.03	−35 26 56.1	1	26.84	S	46.....	3 38 30.57	−35 28 32.8	2	27.21	
11.....	3 38 21.28	−35 27 38.2	2	26.85	S	47.....	3 38 38.51	−35 29 07.9	1	27.24	
12.....	3 38 41.39	−35 31 09.7	1	26.85	S	48.....	3 38 42.16	−35 27 59.6	2	27.24	
13.....	3 38 34.20	−35 24 35.6	1	26.87	S	49.....	3 38 28.89	−35 27 51.1	1	27.25	
14.....	3 38 27.09	−35 25 27.5	2	26.87	S	50.....	3 38 46.92	−35 24 29.9	1	27.27	
15.....	3 38 28.67	−35 27 49.8	1	26.89		51.....	3 38 32.97	−35 25 32.9	2	27.27	
16.....	3 38 33.31	−35 30 32.2	1	26.94	S	52.....	3 38 40.58	−35 30 54.7	1	27.27	
17.....	3 38 36.14	−35 26 11.9	2	26.95	S	53.....	3 38 30.20	−35 28 58.9	2	27.28	
18.....	3 38 27.19	−35 25 13.7	2	26.96	S	54.....	3 38 27.71	−35 26 19.6	1	27.28	
19.....	3 38 21.28	−35 27 15.1	1	26.97	S	55.....	3 38 27.27	−35 24 00.7	1	27.29	
20.....	3 38 24.65	−35 26 27.4	1	26.98	S	56.....	3 38 29.22	−35 26 25.3	1	27.30	
21.....	3 38 39.53	−35 29 21.7	1	26.99	S	57.....	3 38 17.27	−35 24 13.9	1	27.31	
22.....	3 38 14.70	−35 27 03.9	2	27.02	S	58.....	3 38 33.11	−35 28 38.2	2	27.32	
23.....	3 38 46.48	−35 27 24.0	2	27.02	S	59.....	3 38 32.68	−35 29 32.6	1	27.32	
24.....	3 38 35.29	−35 28 09.8	2	27.02	S	60.....	3 38 49.27	−35 25 10.2	1	27.38	
25.....	3 38 34.98	−35 25 53.2	2	27.02	S	61.....	3 38 24.62	−35 25 03.1	1	27.38	
26.....	3 38 23.67	−35 27 12.3	1	27.03	S	62.....	3 38 32.94	−35 25 59.7	2	27.39	
27.....	3 38 42.45	−35 25 13.8	1	27.06	S	63.....	3 38 39.72	−35 24 28.2	1	27.40	
28.....	3 38 23.93	−35 27 43.6	1	27.08	S	64.....	3 38 34.80	−35 23 58.9	1	27.41	
29.....	3 38 19.32	−35 28 17.8	2	27.10	S	65.....	3 38 15.89	−35 29 57.1	1	27.41	
30.....	3 38 32.31	−35 27 32.0	2	27.13		66.....	3 38 23.08	−35 28 22.5	1	27.42	
31.....	3 38 35.20	−35 29 38.7	1	27.13	S	67.....	3 38 13.70	−35 25 41.5	1	27.43	
32.....	3 38 41.40	−35 28 48.3	1	27.14	S	68.....	3 38 41.92	−35 27 55.2	2	27.48	
33.....	3 38 30.73	−35 28 26.7	1	27.14	S	69.....	3 38 40.10	−35 27 43.9	2	27.49	
34.....	3 38 21.46	−35 28 14.0	2	27.15	S	70.....	3 38 34.99	−35 29 28.0	1	27.52	
35.....	3 38 18.02	−35 24 59.5	1	27.15	S	71.....	3 38 18.58	−35 25 27.8	1	27.52	
36.....	3 38 28.51	−35 27 41.5	1	27.16		72.....	3 38 48.16	−35 25 02.3	1	27.57	

TABLE 5

NGC 1404 PLANETARY NEBULAE

ID	α(2000)	δ(2000)	Number	m_{5007}	Sample	ID	α(2000)	δ(2000)	Number	m_{5007}	Sample
1.....	3 38 57.11	−35 35 05.1	1	26.75	S	25.....	3 38 57.39	−35 36 41.0	1	27.36	
2.....	3 38 47.11	−35 34 22.3	1	26.77	S	26.....	3 38 57.00	−35 33 38.9	1	27.37	
3.....	3 38 49.07	−35 35 24.2	1	26.79		27.....	3 38 45.54	−35 36 08.9	1	27.38	
4.....	3 38 52.13	−35 36 39.4	1	26.79	S	28.....	3 38 46.07	−35 36 34.9	1	27.39	
5.....	3 38 48.94	−35 35 22.0	1	26.83		29.....	3 38 52.08	−35 34 45.3	1	27.39	
6.....	3 38 53.19	−35 36 19.9	1	26.90		30.....	3 38 53.29	−35 36 16.4	1	27.41	
7.....	3 38 55.92	−35 35 44.6	1	26.96	S	31.....	3 38 57.19	−35 35 54.8	1	27.42	
8.....	3 38 50.07	−35 35 06.3	1	26.98		32.....	3 38 52.13	−35 34 52.5	1	27.44	
9.....	3 38 52.45	−35 34 31.9	1	26.99	S	33.....	3 38 57.41	−35 34 11.0	1	27.44	
10.....	3 38 46.30	−35 33 59.3	1	27.01	S	34.....	3 38 58.40	−35 35 20.8	1	27.45	
11.....	3 38 59.85	−35 35 51.0	1	27.01	S	35.....	3 38 47.25	−35 36 28.7	1	27.45	
12.....	3 38 57.64	−35 36 34.2	1	27.02	S	36.....	3 38 49.75	−35 34 06.6	1	27.53	
13.....	3 38 54.70	−35 36 29.0	1	27.04	S	37.....	3 38 58.08	−35 33 28.3	1	27.53	
14.....	3 38 48.60	−35 35 55.8	1	27.06	S	38.....	3 38 57.67	−35 36 15.9	1	27.54	
15.....	3 38 54.90	−35 36 24.0	1	27.09	S	39.....	3 38 53.80	−35 35 03.0	1	27.54	
16.....	3 38 58.40	−35 36 33.7	1	27.11	S	40.....	3 38 50.47	−35 34 32.9	1	27.55	
17.....	3 38 53.53	−35 34 57.2	1	27.12	S	41.....	3 38 44.98	−35 36 05.3	1	27.56	
18.....	3 38 50.13	−35 36 12.5	1	27.16		42.....	3 38 47.44	−35 36 34.5	1	27.59	
19.....	3 38 54.16	−35 34 44.4	1	27.18	S	43.....	3 38 59.13	−35 36 30.1	1	27.64	
20.....	3 39 00.21	−35 35 07.3	1	27.21		44.....	3 38 49.51	−35 35 03.8	1	27.68	
21.....	3 38 45.81	−35 34 32.5	1	27.25		45.....	3 38 52.30	−35 33 54.0	1	27.70	
22.....	3 38 57.18	−35 35 10.7	1	27.26		46.....	3 38 55.52	−35 36 36.7	1	27.78	
23.....	3 38 49.83	−35 36 04.2	1	27.32		47.....	3 38 43.53	−35 34 09.6	1	27.98	
24.....	3 38 55.63	−35 35 48.9	1	27.33							

TABLE 6

PN PHOTOMETRIC ERROR VERSUS MAGNITUDE

Magnitude	Mean 1 σ Error	Number
26.65	0.09	3
26.80	0.10	18
26.95	0.12	40
27.10	0.13	36
27.25	0.14	39
27.40	0.15	31
27.55	0.17	16

theoretical limit occurred at $m_{\rm lim} \approx 27.3$, near where the raw PNLFs begin to decrease. To be conservative, we therefore estimate our completeness limit to be $m_{5007} \sim 27.2$; changing this value by 0.1 mag in either direction does not significantly affect any of our results or conclusions.

To confirm this estimate of the completeness limit, we compared the distribution of PNe with $m_{5007} < 27.2$ in NGC 1399 and NGC 1404 with the luminosity profiles of those galaxies. As previous papers in the series have shown, the distribution of PN should roughly follow that of the light; if not, then the PN sample is probably contaminated. To perform this test, the surface photometry of Franx, Illingworth, & Heckman (1989b),

TABLE 7

ASTROMETRIC REFERENCE STARS

Galaxy	ID	α(2000)	δ(2000)
NGC 1316	a	$3^h22^m50^s.37$	−37°12′37″.0
	b	3 22 58.07	−37 11 35.4
	c	3 22 53.89	−37 10 15.4
	d	3 22 49.01	−37 09 26.0
	e	3 22 43.02	−37 09 00.0
	f	3 22 39.66	−37 10 07.8
	g	3 22 38.40	−37 14 45.8
	h	3 22 37.22	−37 14 33.2
	i	3 22 31.66	−37 13 51.7
	j	3 22 25.13	−37 12 47.6
	k	3 22 33.53	−37 15 12.7
	l	3 22 34.89	−37 15 12.5
	m	2 22 23.39	−37 15 43.8
	n	3 22 23.36	−37 14 19.8
	o	3 22 34.51	−37 10 32.7
	p	3 22 34.27	−37 10 02.3
	q	3 22 30.82	−37 10 07.5
	r	3 22 36.53	−37 10 56.3
	s	3 22 45.99	−37 13 15.4
NGC 1399	a	3 38 20.45	−35 27 41.5
	b	3 38 24.81	−35 28 18.2
	c	3 38 28.38	−35 25 39.9
	d	3 38 46.49	−35 25 14.9
	e	3 38 37.06	−35 25 21.9
	f	3 38 31.13	−35 28 10.3
	g	3 38 33.54	−35 24 58.8
	h	3 38 26.84	−35 24 49.1
	i	3 38 33.82	−35 25 57.3
	j	3 38 35.20	−35 27 40.4
	k	3 38 39.26	−35 28 06.3
NGC 1404	a	3 38 43.53	−35 33 49.9
	b	3 38 43.62	−35 35 05.6
	c	3 38 41.71	−35 36 50.5
	d	3 38 41.96	−35 33 13.6
	e	3 38 57.35	−35 34 05.9
	f	3 38 51.32	−35 34 36.3
	g	3 38 50.14	−35 35 32.1
	h	3 38 57.83	−35 34 08.5
	i	3 38 52.60	−35 35 18.9

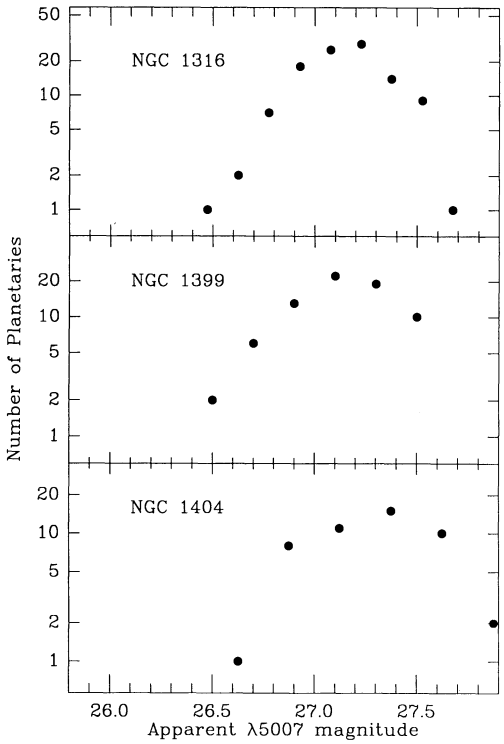

FIG. 3.—The raw planetary nebula luminosity functions of NGC 1316, 1399, and 1404. Magnitudes are defined as in Paper I, where $m_{5007} = -2.5 \log F_{5007} - 13.74$. Although the samples are heterogeneous and contain many objects past the nominal completeness limit of $m_{5007} \sim 27.3$, the similarity in the curves demonstrates that all three galaxies are at about the same distance.

Sparks et al. (1991), Kibblewhite et al. (1989), and Schombert (1986) were used to model each galaxy as a series of concentric elliptical isophotes with varying axial ratios and position angles. The isophotal radial distance of each planetary from the center of its parent galaxy was then calculated by finding the semimajor axis of the isophote upon which it was superposed. The distribution of these distances was compared to the luminosity profile along the major axis of the galaxy, corrected for the fraction of light enclosed in the survey regions. As Figure 4 illustrates, the distribution of PNe in the outer parts of both galaxies does indeed follow the light. In the central regions, PNe are lost due to the bright background of the galaxy; however, once outside the area of incompleteness, our PN sample looks reasonably homogeneous.

4. THE DISTANCE TO THE FORNAX CLUSTER

The PNLF distances to NGC 1316, 1399, and 1404 and their formal uncertainties were calculated by convolving the empirical function

$$N(M) \propto e^{0.307M}[1 - e^{3(M^* - M)}] \qquad (2)$$

with the photometric errors of Table 6 and fitting the resultant curve to the observed PNLFs via the method of maximum likelihood (Ciardullo et al. 1989; Paper II). As in previous papers of the series, we adopted $M^* = -4.48$, based on the Cepheid-based M31 distance of 710 kpc (1986) and foreground extinction of $E(B-V) = 0.11$ (McClure & Racine 1969). With more modern values for M31's distance (770 kpc; Freedman & Madore 1990) and extinction [$E(B-V) = 0.08$; Burstein & Heiles 1984], our distances would increase by ~3%.

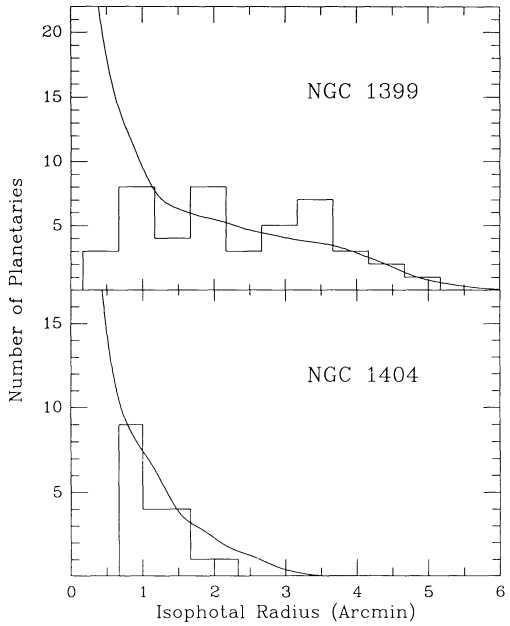

FIG. 4.—Two histograms showing the distribution of isophotal radii for PN candidates in NGC 1399 and NGC 1404 with $m_{5007} < 27.2$. The solid lines display the amount of V luminosity surveyed in each galaxy, again vs. isophotal radius. Within ~60″ in NGC 1399 and ~45″ in NGC 1404 incompleteness is important, as PNe are being lost amid the bright background. Once outside this area, however, the distribution of PNe follows that of the light reasonably well.

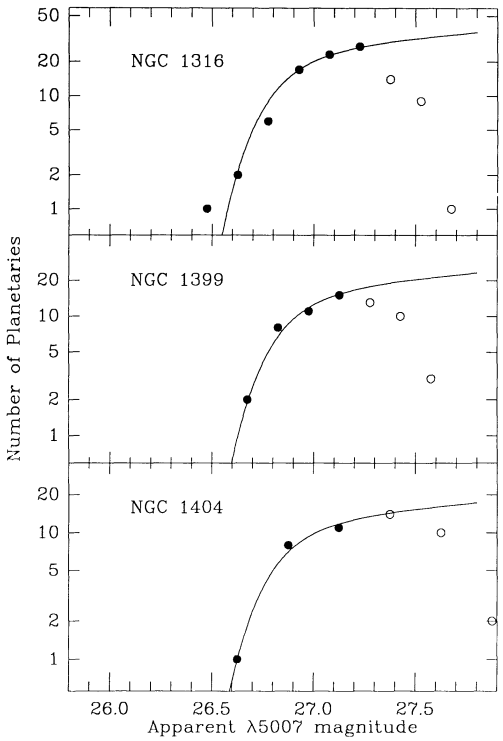

FIG. 5.—The planetary nebula luminosity functions for NGC 1316, 1399, and 1404 derived from complete samples of PNe. The solid lines show the empirical PNLF convolved with the mean photometric error vs. magnitude relation and translated to the most likely apparent distance modulus of each galaxy. Open circles show PNe below the completeness limit which have not been included in the fit.

Before this computation can be performed, however, we need an estimate of the foreground extinction toward Fornax at λ5007 Å. Since the center of the Fornax Cluster has a Galactic latitude of $b^{II} \approx -53°$, we would expect the Galactic extinction in the direction of Fornax to be low, and indeed it is. The global reddening estimates of Sandage (1973), Burstein & McDonald (1975), and de Vaucouleurs, de Vaucouleurs, & Corwin (1976; RC2) all yield $E(B-V)$ values of between 0.006 and 0.051 for the three galaxies considered in this paper, while the reddening maps of Burstein & Heiles (1982) show no evidence of extinction at all in the direction of Fornax. Moreover, the 21 cm based extinction values of Burstein & Heiles (1984) are all negative for the galaxies in question, indicating little, if any, attenuation in their direction. Based on these numbers (and their likely errors), we assumed for our distance calculations a foreground extinction to Fornax of exactly zero. We note, however, that since the total extinction at 5007 Å is given by $A_{5007} = 3.56E(B-V)$ (Seaton 1979), the quoted uncertainty of 0.015 in $E(B-V)$ of the Burstein & Heiles (1984) extinctions propagates directly into an uncertainty of 0.05 mag in the derived distance moduli.

The maximum likelihood fits to our statistical sample of planetaries are summarized in Table 8 and appear in Figure 5. The curves are remarkably similar. NGC 1399, the central galaxy of the cluster, has a most likely distance modulus of 31.17 (17.1 Mpc), with a formal fitting error of +0.05, −0.07. Within the error, NGC 1404's distance modulus is identical, with $\mu = 31.15^{+0.07}_{-0.10}$, and although NGC 1316 is projected well away from the cluster core, it also has the same distance of $\mu = 31.13^{+0.05}_{-0.06}$. This tight clustering is in contrast to the spread in distance seen in Virgo (Paper V), and agrees with the conclusions of Tonry (1991) that Fornax is a very tightly grouped system.

Because the dispersion in distance to our three Fornax gal-

TABLE 8

SUMMARY FOR FORNAX GALAXIES

Parameter	NGC 1316	NGC 1399	NGC 1404
PN magnitude completeness limit	27.2	27.2	27.2
Inner isophotal radius for sample	110″	60″	45″
$V_{sampled}$	9.72	10.46	10.48
m_{bol}	9.02	9.66	10.55
Total number of PNe found	105	72	47
Number of PNe in complete sample	58	37	19
Most likely distance modulus (μ_0)	31.13	31.17	31.15
Most likely distance (Mpc)	16.8 ± 0.4	17.1 ± 0.5	17.0 ± 0.7
Most likely specific PN density ($\alpha_{2.5}$)	10.9×10^{-9}	13.4×10^{-9}	14.8×10^{-9}

axies appears to be small, we can compute an improved distance to the cluster by summing the PN distributions and computing a most likely distance for the entire sample. This is done in Figure 6. From the figure, it is apparent that the PNLF for the three galaxies is exceptionally well-determined and matches the empirical law extremely well. Computed in this way, the most likely distance modulus of Fornax is 31.14 (16.9 Mpc), with a formal uncertainty $+0.03$, -0.04. A Kolmogorov-Smirnov test on the sample shows that the observed PNLF is indistinguishable from that predicted from the empirical law. A power-law luminosity function, such as that proposed by Bottinelli et al. (1991), however, is excluded at the 99% confidence level.

The distance errors quoted above represent only the formal uncertainties associated with the PNLF fitting procedure, not the total error in the computed distances. To obtain the latter quantity, the uncertainty in the maximum likelihood solution must be combined with that of the photometric zero point (0.03 mag), the filter calibration (0.04 mag), the definition of the PNLF (0.05 mag), the distance to M31 (0.10 mag), and the Galactic extinction (0.05 mag). The total error in our distance determination is therefore 0.14 mag.

In addition to the distance modulus, we obtain a second quantity from the fitting of the PNLF: the total PN population within our sampled area. When normalized to the bolometric luminosity, this number becomes α, the luminosity-specific PN density. From theoretical considerations, this quantity, which is related to the galaxy's evolutionary flux and stellar death rate, should be insensitive to galaxy parameters such as age and metallicity (Renzini & Buzzoni 1986). However, as pointed out by Peimbert (1990) and discussed in Hui et al. (1993) and in Paper VII, α does appear to depend on the galaxy color.

In order to normalize our PN number to the total luminosity, we need to know the enclosed bolometric luminosity within the area of completeness in each of our survey fields. For NGC 1399 and 1404, we used the published surface photometry of Franx, Illingworth, & Heckman (1989b), Sparks et al. (1991), Kibblewhite et al. (1989), and Schombert (1986) to sum the total V luminosity contained within our survey fields, excluding the region of incompleteness. We then computed bolometric corrections for the galaxies from the ultraviolet, optical, and infrared colors of Burstein et al. (1988), Poulain (1986, 1988), and Persson, Frogel, & Aaronson (1979) and used these to determine the total bolometric magnitudes listed in Table 8.

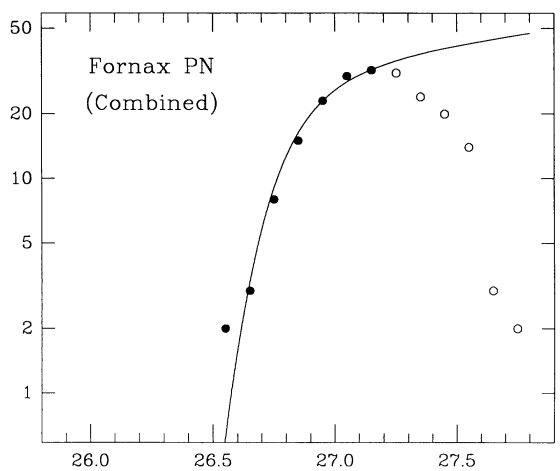

FIG. 6.—The combined PNLF of NGC 1316, 1399, and 1404, excluding those objects outside the regions of completeness. The solid curve is the model PNLF, convolved with the photometric error function and translated to the most likely apparent distance modulus of the cluster. Open circles show PNe below the completeness limit which have not been included in the fit. The data are exceedingly well-fit with the model PNLF, while a power-law luminosity function is excluded at the 99% confidence level.

For NGC 1316, however, this procedure could not be used; while surface photometry is available for the galaxy's inner arcminute (Sparks et al. 1991), our statistical sample does not begin until a radius of 1.8 is reached. To find the luminosity sampled from this galaxy, we used our wide-field summed CCD image from the Tololo Schmidt telescope to measure the total V luminosity on our 4 m frames. After excluding a circular area 1.8 around the nucleus of the galaxy and interpolating over the field stars, we estimated the most probable value for the background sky using areas on the frame far away from any cluster galaxy. We then subtracted this value from the image and summed the remaining counts in those sections of the frame covered by our 4 m image to obtain the instrumental V magnitude of the galaxy. To convert this to a standard magnitude, we determined the B and V magnitudes of five field stars on our frame by comparing their large-aperture instrumental magnitudes with those of 31 Landolt (1973, 1983) standard stars contained on three other Schmidt fields taken during the night. The enclosed V-band galactic luminosity was then calculated by comparing the number of counts enclosed in our survey region to those of two field stars of similar $B-V$ color. To this number, we then added a bolometric correction, determined from the infrared and visual photometry of Persson et al. (1979) and Poulain et al. (1988), to obtain the bolometric magnitude appearing in Table 8.

As a check on this procedure, we also computed NGC 1316's total V magnitude via the same method, but with the inclusion of the central 1.8. The value $V = 8.50$ is entirely in agreement with the value $V = 8.53$ quoted in the RC3 catalog and indicates that our CCD magnitude for the galaxy is accurate.

Figure 7 displays the probability contours of our maximum likelihood solutions for NGC 1316, 1399, and 1404, in both distance modulus and specific PN density. For convenience, as in previous papers of the series, α has been normalized to represent the number of planetaries within 2.5 mag of m^*. A similar plot for the Fornax cluster as a whole appears in Figure 8. The most likely values of μ and α are listed in Table 8.

5. THE FORNAX/VIRGO DISTANCE RATIO

Although the Fornax Cluster is roughly one-seventh the size of Virgo, the structure and galactic populations of the two clusters are similar. This makes the two systems especially amenable to the measurement of their distance ratio, and this number has been computed by several methods. However, before these values can be compared, some discussion is needed about foreground Galactic extinction.

Currently, the extinction estimates commonly used in the literature are those based on H I emission and galaxy counts by Burstein & Heiles (1984). Unfortunately, these may be subject to uncertainties. In the Virgo Cluster core, Burstein & Heiles tabulate B-band extinctions toward 123 objects listed in the atlas of Tully (1988); the average value of these measurements is 0.035 mag, with a formal error of the mean of 0.004 mag. However, for Fornax, the average Burstein & Heiles extinction to 21 galaxies is $A_B = -0.071 \pm 0.006$ (error of the mean). This negative value may arise from an abnormally high

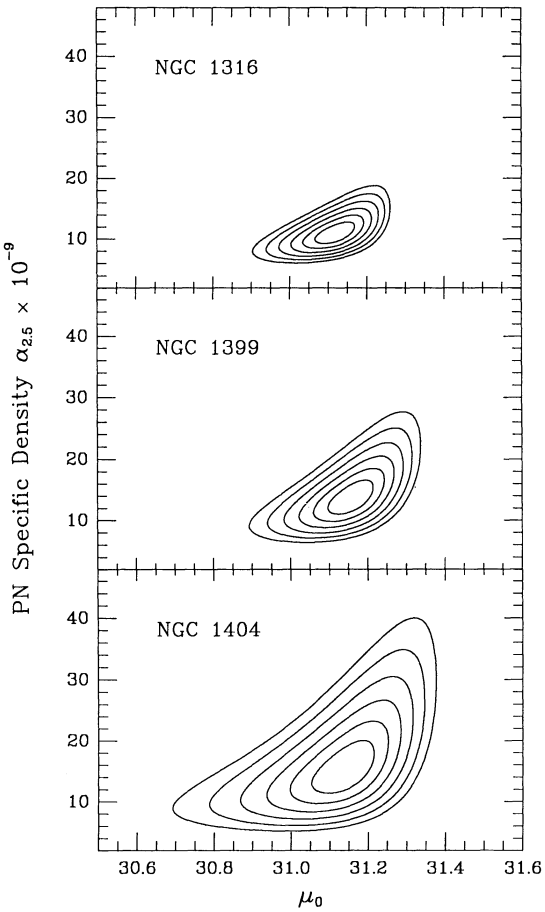

FIG. 7.—Maximum likelihood confidence contours for NGC 1316, 1399, and 1404 derived from fitting the empirical PNLF (convolved with the photometric error function) to complete samples of PNe in each galaxy. The abscissa is the true distance modulus; the ordinate is the number of PNe within 2.5 mag of the magnitude cutoff, normalized to the amount of bolometric luminosity surveyed. We have assumed that there is no foreground extinction to the galaxies. The contours of probability (shown at intervals of 0.5 σ) arise from the uncertainty in fitting the model PNLF to the observed PNLF: horizontal errors reflect the uncertainty in the fitting the distance modulus, whereas vertical errors are caused by uncertainties in normalizing to the observed number of PNe.

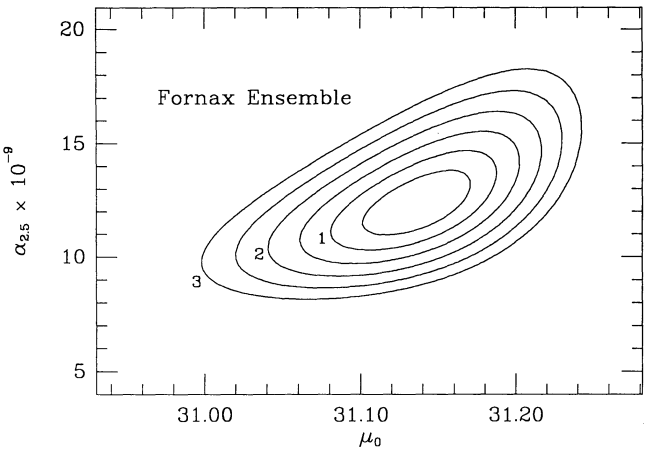

FIG. 8.—The maximum likelihood probability contours for the 114 PNe in the statistical sample shown in Fig. 6. Note the extreme precision to which the centroid of the contours can be determined. The 1 σ uncertainty of the fit is only 0.07 mag in the distance modulus, which corresponds to an uncertainty of $\pm 3\%$ in the distance.

gas-to-dust ratio in the region, and makes a reliable comparison of the extinction to the two clusters especially difficult. This being the case, in our comparison we adopt extinctions to the two clusters that are identically zero. Note that if we were to adopt 0.035 mag as the B-band extinction to Virgo and treat the Fornax reddening as zero (as recommended by Burstein & Heiles), our derived Fornax/Virgo distance ratio would increase by only 1%.

Under the zero reddening assumption, Table 9 compares our Fornax/Virgo distance ratio to those derived from other techniques. The upper part of the table shows results from methods which require a galaxy sample essentially different from our own: spiral galaxies for the IR Tully-Fisher relation, dwarf ellipticals for the surface-brightness method of Bothun, Caldwell, & Schombert (1989), a broad range of Hubble types for the work of Ferguson & Sandage (1988), and the galaxies NGC 1316 and NGC 4419 for SNe Ia. A more complete comparison of PNLF and SN Ia distances will soon be possible for a number of galaxies, but for the present we have simplified the comparison by using one presumed core galaxy from each cluster. For all these methods we have simply compared the average cluster distance modulus given by the authors with our own mean cluster distance.

The methods listed in the lower part of Table 9 cover a sample of ellipticals similar to our own; for each of these, we have recomputed our average distance using only galaxies common to both samples. For the globular cluster luminosity function (GCLF), the galaxies we used for comparison are NGC 1399 in Fornax and NGC 4486, 4649, and 4472 in Virgo. (The distance ratio given by Bridges, Hanes, & Harris 1991 also included NGC 4365, but since that galaxy has a small globular cluster population (Harris et al. 1991), its contribution to the total Virgo GCLF is negligible.) For the D_n-σ relation,

TABLE 9

FORNAX/VIRGO DISTANCE COMPARISON

Method	$\mu_{For}-\mu_{Vir}$	PNLF $\mu_{For}-\mu_{Vir}$
IRTF (Aaronson et al. 1989)	-0.25 ± 0.23	$+0.24 \pm 0.10$
dE galaxies (Bothun, Caldwell, & Schombert 1989)	-0.16 ± 0.16	$+0.24 \pm 0.10$
L-Σ (Ferguson & Sandage 1988)	$+0.00 \pm 0.22$	$+0.24 \pm 0.10$
Type Ia SNe (Hamuy et al. 1991)	$+0.09 \pm 0.14$	$+0.24 \pm 0.10$
GCLF (Bridges, Hanes, & Harris 1991)	-0.01 ± 0.46	$+0.31 \pm 0.12$
D_n-σ (Faber et al. 1989)	$+0.25 \pm 0.31$	$+0.31 \pm 0.11$
SBF (Tonry 1991)	$+0.08 \pm 0.11$	$+0.29 \pm 0.10$

our numbers reflect the averages of seven galaxies: NGC 1399 and 1404 in Fornax and NGC 4374, 4406, 4472, 4486, and 4649 in Virgo. The same seven galaxies, along with NGC 1316, are also used in our comparison with the surface brightness fluctuation (SBF) method.

As Table 9 shows, the PNLF method has a small internal error and produces a Fornax/Virgo distance ratio somewhat larger than that found by the other methods, although the measurement is still consistent within the errors. Two of the methods (IR Tully-Fisher and dwarf ellipticals) explicitly disagree with the PNLF distance ratio. However, the Tully-Fisher relation uses spiral galaxies, which are further from the cluster cores and may be contaminated by background members (Pierce & Tully 1988; Teerikorpi et al. 1992), and the dwarf elliptical surface brightness method has not been used extensively as a distance estimator. The methods claiming the lowest errors (type Ia SNe and surface brightness fluctuations) agree more closely with our results.

6. DISCUSSION

With the addition of NGC 1316, 1399, and 1404, the number of galaxies with PNLF distance determinations has grown sufficiently large that it is possible to perform global comparisons with other methods and test for the presence of systematic errors. A detailed comparison with the surface brightness fluctuation method has recently been presented by Ciardullo, Jacoby, & Tonry (1993); a similar comparison with the D_n-σ relation is also possible.

Figure 9 plots distances measured with the D_n-σ relation (Faber et al. 1989) against our PNLF distances for three galaxies in Fornax (this paper), five galaxies in Virgo (Paper V), two galaxies in the Leo I Group (Paper IV; Ciardullo, Jacoby, & Ford 1989), and the field S0 galaxy NGC 3115. To facilitate the comparison, the PNLF distances have been revised to match the extinction values used in the determination of D_n. The best fitting line has a slope of 91 ± 28 km s^{-1} Mpc^{-1}, while the scatter about this line is 0.34 mag in distance

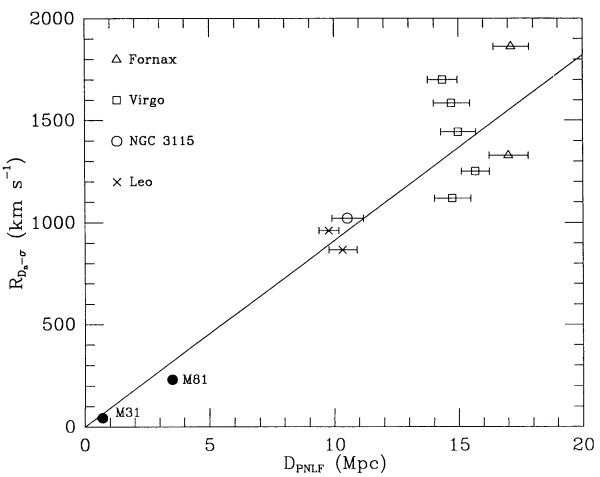

FIG. 9.—A comparison of PNLF distances with those derived from the D_n-σ method. Open circles are measurements of elliptical and S0 galaxies from Faber et al. (1989); the solid points, which are shown for illustrative purposes only, are the spiral calibrators of Dressler (1987). The error bars represent the formal uncertainties in the PNLF fits. A regression through zero has a most likely slope of 91 ± 28 km s^{-1} Mpc^{-1}; the scatter about the line is 0.34 mag. The data suggest that the error estimates for the both the PNLF and D_n-σ method are reasonable.

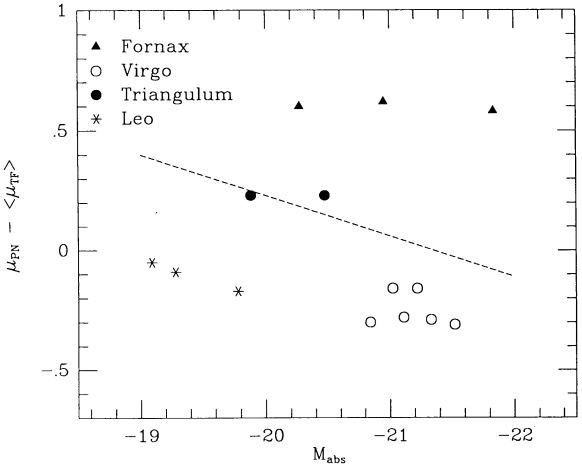

FIG. 10.—The individual PNLF distance modulus minus Tully-Fisher group distance modulus for galaxies in the Fornax, Virgo, Triangulum (NGC 1023), and Leo I Groups as a function of absolute B magnitude. The dashed line shows the slope of the correlation proposed by Bottinelli et al. (1991), which is not supported by the data. The depth of the Virgo Cluster is clearly apparent.

modulus. As discussed above, the errors in the PNLF measurements are estimated at 0.10 mag, while Jacoby et al. (1992) predict an error of 0.45 mag for the D_n-σ relation. Within the 90% confidence level, the observed scatter is consistent with the prediction of 0.46 mag for the dispersion between the two methods; if anything, the quoted errors for the two methods may be overestimated.

Bottinelli et al. (1991) have questioned the reliability of the PNLF distance measurements by proposing the existence of a correlation between galaxy luminosity and PNLF distance. Figure 10 shows a comparison of these parameters for galaxies of four clusters; Fornax (this paper); Virgo (Paper V); the Leo I Group (Paper IV); and the Triangulum Spur, or NGC 1023 Group (Paper VII). The ordinate of the plot shows the PNLF distance moduli for individual galaxies minus a mean Tully-Fisher distance to each group. These group distances are based on four galaxies in Fornax (NGC 1326, 1365, 1406, and 1425), NGC 3368 in Leo, and NGC 891 in Triangulum (Bottinelli et al. 1985). The Virgo distance is taken at 16.5 Mpc, based on the analysis in Teerikorpi et al. (1992). The dashed line shows the slope of the proposed correlation between luminosity and PNLF distance. An error in the Tully-Fisher cluster distances could move any group of points up or down on the plot but would not change the relationships between points within a group.

The plot shows, as found by Tonry (1991), that the Fornax core is extremely tight, while the Virgo cluster has significant depth. NGC 4406 and NGC 4374 lie somewhat beyond the rest of the Virgo core. NGC 1023 and NGC 891 are found at the same distance despite their differing magnitudes and Hubble types. Only among the three members of Leo I is there any trend of distance with absolute magnitude. However, the members of Fornax, with their similar distances and large spread in absolute magnitude, give strong evidence against the existence of a correlation.

Using the distance measured with the PNLF, it is also possible to begin a calibration of a longer range distance indicator: Type Ia SNe. In 1980 and 1981, two SNe Ia (1980N and 1981D) were observed just 3 months apart in NGC 1316. Photographic and photoelectric UBV photometry published by

Hamuy et al. (1991) show that the two SNe had extremely similar light and color curves, which were also very much like those of the SN Ia prototype SN 1981B in Virgo. The infrared *JHK* observations of Elias et al. (1985) were also very consistent between the two. SN 1980N and SN 1981D had maximum magnitudes of 12.48 and 12.40, respectively, in V and 13.31 and 13.35 in H. With our measured distance to NGC 1316 of 16.9 Mpc, this yields average absolute peak magnitudes of -18.65 in V and -17.8 in H. The V-band value is in good agreement with Pierce, Ressler, & Shure's (1992) calibration of 1937C but is 1 mag fainter than the calibration by Sandage et al. (1992). It is still unclear how large the intrinsic dispersion in SN Ia peak magnitudes might be (Phillips 1993), but finding more accurate distances to galaxies that also hosted well-observed SNe is crucial to the calibration of SNe Ia as distance indicators and also to the understanding of SNe in general. We hope to use the PNLF to study several more SN galaxies in the near future.

7. THE HUBBLE CONSTANT

In Paper V, we estimated a value for the Hubble constant based on a PNLF distance to the Virgo Cluster. However, Virgo is not the ideal location to perform this measurement; because the line-of-sight depth of the cluster is significant (even for the core ellipticals), it is difficult to assign a single distance to the cluster (Paper V; Tonry, Ajhar, & Luppino 1990; Jacoby et al. 1992). Fornax, however, is a tightly grouped system, as our measurements and the measurements of Tonry (1991) demonstrate. Thus, it is a much cleaner group to use for a measurement of the Hubble constant.

While it is possible to obtain the Hubble constant directly from Fornax, uncertainties in the local velocity field limit the usefulness of this type of determination. A more secure route to H_0, which avoids the problems of local peculiar velocities, comes from scaling from Fornax galaxies to the galaxies of Coma. From the D_n-σ relation, the distance ratio between Coma and Fornax is 5.25 ± 0.38 (Faber et al. 1989). If the velocity of Coma in the microwave background frame is 7185 ± 60 km s^{-1} (Faber et al. 1989, corrected by Smoot et al. 1991), then our distance to Fornax implies a Hubble constant of $H_0 = 81 \pm 8$ km s^{-1} Mpc^{-1}. Similarly, if we use the Coma-Fornax distance ratio of 6.14 ± 0.63 found by Aaronson et al. (1989) from the IR Tully-Fisher relation, then the estimated Hubble constant becomes $H_0 = 69 \pm 8$ km s^{-1} Mpc^{-1}. Our combined value of $H_0 \approx 75 \pm 8$ km s^{-1} Mpc^{-1} from Fornax is thus in excellent agreement with that computed from the Virgo PNLF distance measurements (Paper V).

We would like to thank Mark Phillips for his valuable assistance during our December 1991 run. This work was supported in part by NASA grant NAGW-3159 and NSF grant AST92-57833.

REFERENCES

Aaronson, M., et al. 1989, ApJ, 338, 654
Allen, C. W. 1976, Astrophysical Quantities (London: Athlone)
Bothun, G. D., Caldwell, N., & Schombert, J. M. 1989, AJ, 98, 1542
Bottinelli, L., Gouguenheim, L., Paturel, G., & de Vaucouleurs, G. 1985, A&AS, 59, 43
Bottinelli, L., Gouguenheim, L., Paturel, G., & Teerikorpi, P. 1991, A&A, 252, 550
Bridges, T. J., Hanes, D. A., & Harris, W. E. 1991, AJ, 101, 469
Burstein, D., Bertola, F., Buson, L. M., Faber, S. M., & Lauer, T. D. 1988, ApJ, 328, 440
Burstein, D., & Heiles, C. 1982, AJ, 87, 1165
———. 1984, ApJS, 54, 33
Burstein, D., & McDonald, L. H. 1975, AJ, 80, 17
Ciardullo, R., Ford, H. C., Neill, J. D., Jacoby, G. H., & Shafter, A. W. 1987, ApJ, 318, 520
Ciardullo, R., & Jacoby, G. H. 1992, ApJ, 388, 268 (Paper VIII)
Ciardullo, R., Jacoby, G. H., & Ford, H. C. 1989, ApJ, 344, 715 (Paper IV)
Ciardullo, R., Jacoby, G. H., Ford, H. C., & Neill, J. D. 1989, ApJ, 339, 53 (Paper II)
Ciardullo, R., Jacoby, G. H., & Harris, W. E. 1991, ApJ, 383, 487 (Paper VII)
Ciardullo, R., Jacoby, G. H., & Dejonghe, H., 1993, ApJ, 414, 454
Davies, R. L., Burstein, D., Dressler, A., Faber, S. M., Lynden-Bell, D., Terlevich, R. J., & Wegner, G. 1987, ApJS, 64, 581
de Vaucouleurs, G., de Vaucouleurs, A., & Corwin, H. G., Jr. 1976, Second Reference Catalog of Bright Galaxies (Austin: Univ. of Texas Press) (RC2)
de Vaucouleurs, G., de Vaucouleurs, A., Corwin, H. G., Jr., Buta, R. J., Paturel, G., & Fouqué, P. 1991, Third Reference Catalog of Bright Galaxies (New York: Springer) (RC3)
Dressler, A. 1987, ApJ, 317, 1
Elias, J. H., Matthews, K., Neugebauer, G., & Persson, S. E. 1985, ApJ, 296, 379
Faber, S. M., Wegner, G., Burstein, D., Davies, R. L., Dressler, A., Lynden-Bell, D., & Terlevich, R. J. 1989, ApJS, 69, 763
Ferguson, H. C., & Sandage, A. 1988, AJ, 96, 1520
Franx, M., Illingworth, G., & Heckman, T. 1989a, ApJ, 344, 613
———. 1989b, AJ, 98, 538
Freedman, W. L., & Madore, B. F. 1990, ApJ, 365, 186
Gorgas, J., Efstathiou, G., & Salamanca, A. A. 1990, MNRAS, 245, 217
Hamuy, M., Phillips, M. M., Maza, J., Wischnjewsky, M., Uomoto, A., Landolt, A. U., & Khatwani, R. 1991, AJ, 102, 208
Harris, W. E., Allwright, J. W. B., Pritchet, C. J., & van den Bergh, S. 1991, ApJS, 76, 115
Hui, X., Ford., H. C., Ciardullo, R., & Jacoby, G. H. 1993, ApJS, 88, 000
Jacoby, G. H., et al. 1992, PASP, 104, 599
Jacoby, G. H., Ciardullo, R., & Ford, H. C. 1990, ApJ, 356, 332 (Paper V)
Jacoby, G. H., Ciardullo, R., Ford, H. C., & Booth, J. 1989, ApJ, 344, 704 (Paper III)
Jacoby, G. H., Quigley, R. J., & Africano, J. L. 1987, PASP, 99, 672
Jenkins, C. R., & Scheuer, P. A. G. 1980, MNRAS, 192, 595
Kibblewhite, E. J., Cawson, M. G. M., Phillipps, S., Davies, J. I., & Disney, M. J. 1989, MNRAS, 236, 187
Landolt, A. U. 1973, AJ, 78, 959
———. 1983, AJ, 88, 439
McClure, R. D., & Racine, R. 1969, AJ, 74, 1000
Oke, J. B. 1974, ApJS, 27, 21
Peimbert, M. 1990, Rev. Mexicana Astron. Af., 20, 119
Persson, S. E., Frogel, J. A., & Aaronson, M. 1979, ApJS, 39, 61
Phillips, M. M. 1993, private communication
Pierce, M. J., Ressler, M. E., & Shure, M. S. 1992, ApJ, 390, L45
Pierce, M. J., & Tully, R. B. 1988, ApJ, 330, 579
Poulain, P. 1986, A&AS, 64, 225
———. 1988, A&AS, 72, 215
Renzini, A., & Buzzoni, A. 1986, in Spectral Evolution of Galaxies, ed. C. Chiosi & A. Renzini (Dordrecht: Reidel), 195
Sandage, A. 1973, ApJ, 183, 711
Sandage, A., Saha, A., Tammann, G. A., Panagia, N., & Macchetto, D. 1992, ApJ, 401, L7
Sandage, A., & Tammann, G. A. 1981, A Revised Shapley-Ames Catalog of Bright Galaxies (Washington: Carnegie Institution of Washington) (RSA)
Schombert, J. M. 1986, ApJS, 60, 603
Schweizer, F. 1980, ApJ, 237, 303
Seaton, M. J. 1979, MNRAS, 187, 73P
Smoot, G. F., et al. 1991, ApJ, 371, L1
Sparks, W. B., Wall, J. V., Jorden, P. R., Thorne, D. J., & van Breda, I. 1991, ApJS, 76, 471
Stetson, P. B. 1987, PASP, 99, 191
Stone, R. P. S. 1977, ApJ, 218, 767
Stone, R. P. S., & Baldwin, J. A. 1983, MNRAS, 204, 347
Teerikorpi, P., Bottinelli, L., Gouguenheim, L., & Paturel, G. 1992, A&A, 260, 17
Tonry, J. L. 1991, ApJ, 373, L1
Tonry, J. L., Ajhar, E. A., & Luppino, G. A. 1990, AJ, 100, 1416
Tully, R. B. 1988, Nearby Galaxies Catalog (Cambridge: Cambridge University Press)